Ground State of Liquid Helium—Boson Solutions for Mass 3 and 4†

WALTER E. MASSEY*
Arthur H. Compton Laboratory of Physics, Washington University, Saint Louis, Missouri
(Received 9 June 1966)

The ground-state properties of a system of liquid He^4 and of an artificial mass-3 boson system are calculated by a variational procedure employing a Jastrow-type trial wave function in conjunction with the Kirkwood superposition approximation for the three-particle distribution function. The parameters in a Lennard-Jones 6–12 potential are determined in a self-consistent manner and the energy, pressure, velocity of sound, pair-distribution function, and liquid-structure function are calculated as functions of density. The agreement between the theoretical and experimental results is good.

INTRODUCTION

THE ground-state properties of a boson liquid can be calculated by a systematic procedure employing a Jastrow-type trial wave function in conjunction with the Kirkwood superposition approximation for the three-particle distribution function. The calculation employs a variational process in which the pair-distribution function is the varied quantity. The Bogoliulov-Born-Green-Kirkwood-Yvon (BBGKY) equation is used to provide a one-to-one correspondence between a pair-distribution function and a Jastrow-type wave function. The procedure yields unambiguous results in the sense that the optimum pair-distribution function determined by finding the minimum value of the total energy satisfies all available necessary conditions implied by the connection between a pair-distribution function and a many-particle wave function.

The calculation of the ground-state properties of liquid He^4 and the ground-state properties of an artificial mass-3 boson system interacting through the same potential is reported in this paper. The potential is a Lennard-Jones 6–12 potential the parameters of which are calculated in a self-consistent manner.

The mass-3 boson results are needed in a calculation of the ground-state properties of liquid He^3 by the method of correlated basis functions.[1–3]

BASIC RELATIONS

Consider a system of N spinless bosons in a volume Ω with the Hamiltonian

$$H=-\frac{\hbar^2}{2M}\sum_{i=1}^{N}\Delta_i+V(\mathbf{r}_1,\mathbf{r}_2,\cdots\mathbf{r}_N). \tag{1}$$

Of interest here are the ground-state properties of this system in the limit $N\to\infty$, $\Omega\to\infty$, while the density $\rho=N/\Omega$ is held constant.

The two- and three-particle distribution functions are useful in describing the properties of such a system. These functions are defined in terms of the trial function, $\Psi(\mathbf{r}_1,\mathbf{r}_2,\cdots\mathbf{r}_N)$ as follows: The two-particle function is given by

$$P^{(2)}(r_{12})\equiv\rho^2 g(r_{12})=\frac{N(N-1)\int|\Psi(\mathbf{r}_1,\cdots\mathbf{r}_N)|^2 d\mathbf{r}_3\cdots d\mathbf{r}_N}{\int|\Psi(\mathbf{r}_1,\cdots\mathbf{r}_N)|^2 d\mathbf{r}_1\cdots d\mathbf{r}_N} \tag{2}$$

and the three-particle function by

$$P^{(3)}(1,2,3)\equiv\rho^3 g^{(3)}(1,2,3)=\frac{N(N-1)(N-2)\int|\Psi(\mathbf{r}_1,\cdots\mathbf{r}_N)|^2 d\mathbf{r}_4\cdots d\mathbf{r}_N}{\int|\Psi(\mathbf{r}_1,\cdots\mathbf{r}_N)|^2 d\mathbf{r}_1\cdots d\mathbf{r}_N}. \tag{3}$$

$g(r)$ is the "radial" or "pair" distribution function which is directly related to the experimentally measurable liquid-structure function $S(k)$. The normalization of $g(r)$ as determined from (2) is

$$\rho\int[g(r)-1]d\mathbf{r}=-1, \tag{4}$$

where it is assumed that $g(\infty)=1$. The liquid-structure function can be written

$$S(k)=1+\rho\int[g(r)-1]e^{i\mathbf{k}\cdot\mathbf{r}}d\mathbf{r}. \tag{5}$$

A trial wave function of the Bijl-Dingle-Jastrow[4] (BDJ) type:

$$\Psi(\mathbf{r}_1,\cdots\mathbf{r}_N)=\prod_{i<j}e^{\frac{1}{2}u(r_{ij})} \tag{6}$$

is assumed for the ground state of the system. The potential is taken to be a sum of two-body interactions

$$V(\mathbf{r}_1,\mathbf{r}_2,\cdots\mathbf{r}_N)=\sum_{i<j}v(r_{ij}), \tag{7}$$

where $v(r)$ is a Lennard-Jones (L-J) 6-l function. For such a potential the boundary conditions on $u(r)$ and

* Present address: Solid State Science Division, Argonne National Laboratory, Argonne, Illinois.
† Supported in part by the U. S. Air Force Office of Scientific Research under Grant No. AFOSR-62-412 and the National Science Foundation under Grant No. SP-3211.
[1] F. Y., Wu and E. Feenberg, Phys. Rev. 128, 943 (1962).
[2] E. Feenberg and C. W. Woo, Phys. Rev. 137, A391 (1965).
[3] C. W. Woo, Phys. Rev. (to be published).
[4] R. Jastrow, in *The Many-Body Problem*, edited by J. Percus (Interscience Publishers, Inc., New York, 1963).

$g(r)$ are

$$u(r)=-\infty \quad \text{at} \quad r=0, \qquad u(r)=0 \quad \text{at} \quad r=\infty, \tag{8}$$

and

$$g(r)=0 \quad \text{at} \quad r=0, \qquad g(r)=1 \quad \text{at} \quad r=\infty. \tag{9}$$

Using Eqs. (6) and (2) the expectation value of the Hamiltonian in the ground state can be expressed in terms of $g(r)$ and $u(r)$ as

$$\langle H\rangle=\langle T\rangle+\langle V\rangle,$$
$$\langle T\rangle=N\rho(\hbar^2/8M)\int g'(r)u'(r)d\mathbf{r}, \tag{10}$$
$$\langle V\rangle=\tfrac{1}{2}N\rho\int g(r)v(r)d\mathbf{r},$$

(the prime denotes differentiation). If $g(r)$ is known, $\langle V\rangle$ can be calculated immediately; however, the correlation function $u(r)$ must also be known to calculate $\langle T\rangle$. The BBGKY equation[5] in the form

$$g'(r_{12})=g(r_{12})u'(r_{12}) +\rho\int[g_k^{(3)}(1,2,3)-g(r_{12})g(r_{13})]\cos(12,13)d\mathbf{r}_3 \tag{11}$$

can be used to derive a $u(r)$ from a given $g(r)$. The function $g_k^{(3)}(1,2,3)$ is the Kirkwood superposition approximation (KSA) for the three-particle distribution function:

$$g_k^{(3)}(1,2,3)=g(r_{12})g(r_{13})g(r_{23}). \tag{12}$$

A discussion of the accuracy of the KSA as applied to liquid He^4 and a comparison with an alternative approximation for the three-particle distribution function has been given by Jackson.[6]

Abe,[7,8] who first applied Eq. (11) to calculate the ground-state properties of liquid He^4, obtained an approximate solution to the equation and used an experimentally determined $g(r)$ in his evaluation of $\langle H\rangle$. Abe's approximation [giving $u(r)$ as a functional in $g(r)$] was later recognized as being identical with the hypernetted-chain approximation.

Wu and Feenberg[5] (WF) calculated the ground-state energy of liquid He^4 by solving Eq. (11) exactly on a high-speed computer. They also used an experimental $g(r)$. The accuracy of calculations which use experimentally determined pair-distribution functions is limited by the lack of knowledge of $g(r)$ for very small and very large values of the variable r. The directly measured quantity is the liquid-structure function $S(k)$. This function has not been measured over a sufficiently large range of k values to allow an accurate determination of $g(r)$.[9,10] Furthermore, experimental data are available only over a limited range of pressures and only for temperatures above 1°K.

Using the BBGKY equation the expectation value of the kinetic energy is written

$$\langle T\rangle=N\rho(\hbar^2/8M)(J_a+J_b), \tag{13}$$

$$J_a=\int([g'(r)]^2/g(r))d\mathbf{r},$$

$$J_b=-\rho\int g'(r_{12})d\mathbf{r}_2\int[g(r_{23})-1]g(r_{13})u'(r_{13}) \times\cos(12,13)d\mathbf{r}_3. \tag{14}$$

This division is useful in estimating the accuracy of the calculation. All the uncertainty introduced into $\langle T\rangle$ by the use of the KSA is contained in the term J_b.

An extremum principle introduced by Wu and Feenberg[5] is useful in devising a rapid numerical method for solving the BBGKY equation. Equation (11) is the Euler-Lagrange equation for the functional

$$J=-\int g(r_{12})[u'(r_{12})]^2d\mathbf{r}_2+2\int g'(r_{12})u'(r_{12})d\mathbf{r}_2 -\rho\int g(r_{12})g(r_{23})g(r_{31})u'(r_{12})u'(r_{13}) \times\cos(12,13)d\mathbf{r}_2d\mathbf{r}_3. \tag{15}$$

The extreme value

$$J_{\text{ext}}=\int g'(r)u'(r)d\mathbf{r} \tag{16}$$

is attained when $u(r)$ satisfies Eq. (11); consequently

$$\langle T\rangle=N\rho(\hbar/8M)J_{\text{ext}}. \tag{17}$$

Thus the expectation value of the kinetic energy is expressed in terms of the extreme value of J.

A description of how this extremum principle is used in this calculation to solve the BBGKY equation is given in Appendix A.

Application of the virial theorem[5] yields the equation

$$P=\tfrac{2}{3}\langle T\rangle/N-\tfrac{1}{6}\rho^2\int g(r)rv'(r)d\mathbf{r}, \tag{18}$$

giving the pressure in terms of the pair-distribution function $g(r)$. For a Lennard-Jones 6-l potential,

$$v(r)=\epsilon^*/(l-6)[6(r^*/r)^l-l(r^*/r)^6], \tag{19}$$

[5] F. Y. Wu and E. Feenberg, Phys. Rev. **122**, 739 (1961).
[6] H. W. Jackson, Ph.D. thesis, Washington University, 1963 (unpublished).
[7] R. Abe, Progr. Theoret. Phys. (Kyoto) **19**, 57 (1958).
[8] R. Abe, Progr. Theoret. Phys. (Kyoto) **19**, 407 (1958).
[9] D. Henshaw, Phys. Rev. **119**, 14 (1960).
[10] W. Gordon, C. Shaw, and J. Daunt, Phys. Rev. **96**, 1444 (1954).

Eq. (18) becomes

$$P=\tfrac{2}{3}\langle T\rangle/N-\frac{1}{3}\frac{\epsilon^*}{(l-6)}(6lr^{*l}C_l-6lr^{*6}C_6), \quad (20)$$

where

$$C_m=2\pi\rho\int_0^\infty g(r)r^{2-m}dr. \quad (21)$$

In terms of the C_m, $\langle H\rangle$ is given by

$$\langle H\rangle/N=\langle T\rangle/N+[\epsilon^*/(l-6)][6r^{*l}C_l-lr^{*6}C_6]. \quad (22)$$

Method of Calculation

The calculation begins with the construction of a family of trial functions $g(r,\alpha_i)$ representing possible approximate pair-distribution functions. The trial functions are parametrized by the set of variables α_i, $i=1, 2, \cdots s$. The BBGKY equation provides a relation between a $g(r,\alpha_i)$ of this family and a BDJ-type wave function. The expectation value of the Hamiltonian is expressed in terms of $g(r,\alpha_i)$ and $u(r,\alpha_i)$ as shown in Eq. (10). A best pair-distribution function, the corresponding best $u(r,\alpha_i)$ and best value of the energy are all determined by the minimum value of $\langle H\rangle$ in the α_i parameter space.

The parameters α_i are thus determined by the s equations

$$\left.\frac{\partial\langle H(\alpha_i)\rangle}{\partial\alpha_i}\right|_{\alpha_i=\bar{\alpha}_i}=0, \quad i=1, 2, \cdots, s, \quad (23)$$

where $\bar{\alpha}_i$ is the optimum set of the parameters.

The parameters ϵ^* and r^* in the Lennard-Jones potential are determined in a self-consistent manner so that the minimum energy as a function of density and the associated density coincide with the experimental values for liquid He^4 at $T=0$°K. Equations (20) and (22) with $p=0$ atm, $\rho=\rho_0$ and $\langle H(\bar{\alpha}_i)\rangle=\epsilon_0 N$ (ϵ_0 and ρ_0 being the experimental values of the ground-state energy per particle and the equlibrium density for liquid He^4 at $T=0$°K) along with Eq. (23), provide a set of $s+2$ equations which are solved simultaneously to yield ϵ^*, r^* and the optimum set of s variational parameters $\bar{\alpha}_i$. Because of the complexity of the equations, the solutions must be found by an iteration procedure in which ϵ^* and r^* are initially assumed known. Here the values determined by gas phase calculations provide an initial input.

Once ϵ^* and r^* are known the variational procedure [the solution of Eq. (23)] is repeated at different densities to yield the ground-state energy as a function of density. From this "equation of state at $T=0$°K," the pressure, compressibility, and velocity of sound are calculated as functions of density. The optimum pair-distribution function, liquid-structure function, and correlation function are automatically obtained at each density.

The potential determined for He^4 is also assumed to be appropriate for the description of an artificial mass-3 boson system. The ground-state properties at mass 3 are computed as described above except that the interaction constants ϵ^* and r^* are not varied.

RESULTS: MASS 4

The explicit formula for the family of trial functions used in the calculations is

$$g(r)=g_0(r)+\delta g_1(r), \quad (24)$$

where

(a) $g_0(r)=(C+1)\exp[-(d/r)^{10}]-C\times\exp[-(1+z)(d/r)^{10}]$

and

(b) $\delta g_1(r)=A\{(d/r)^m\exp[-(1+y)(d/r)^{10}]-B(d/r)^n\exp[-(1+q)(d/r)^{10}]\}$.

The parameters in the set α_i are $\eta=2\pi\rho d^3$, z, A, y, q, m, n. The parameters C and B are fixed by the normalization condition [Eq. (4)] in the form

$$\rho\int[g_0(r)-1]d\mathbf{r}=-1 \quad (25)$$

and

$$\int\delta g_1(r)d\mathbf{r}=0. \quad (26)$$

Equations (25) and (26) yield

$$C=(1.155574/\eta-1)/[1-(1+z)^{0.3}] \quad (27)$$

and

$$B=\frac{\Gamma((m-3)/10)(1+q)^{(n-3)/10}}{\Gamma((n-3)/10)(1+y)^{(m-3)/10}}. \quad (28)$$

The exponential factor in the trial function is suggested by the analytical form which fits the first rising slope of the experimental $g(r)$[5].

Only those $g(r,\alpha_i)$ which satisfy the following conditions are considered as trial pair-distribution functions:

$$\begin{aligned}&\text{(a)}\quad g(r)\geqslant 0 \quad \text{for} \quad 0\leq r\leq\infty;\\ &\text{(b)}\quad S(k)\geqslant 0, \quad \text{for} \quad 0\leqslant k\leq\infty;\\ &\text{(c)}\quad S(0)=0;\\ &\text{(d)}\quad 4\pi\rho^{2/3}\int_0^\infty[1-g(r)]rdr\leq 2.8887.\end{aligned} \quad (29)$$

Conditions (a), (b), and (c) are obvious physical requirements. Condition (d) is the "Coulomb inequality" recently derived by Feenberg.[11] A pair-distribution function which does not satisfy (d) cannot be generated by a wave function. This condition is useful here since the wave function generated from $g(r)$ by

[11] E. Feenberg, J. Math. Phys. **6**, 658 (1965).

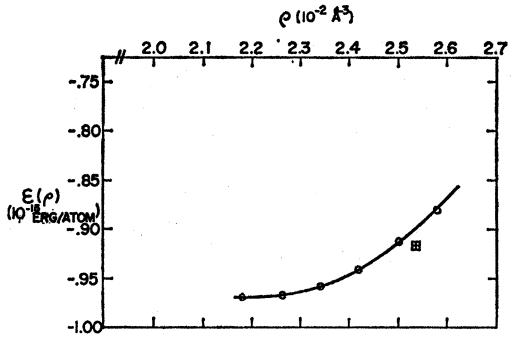

FIG. 1. Ground-state energy per particle as a function of density for the mass-4 system, ⊠ = experimental energy at $P=25$ atm.

way of an approximate equation need not necessarily be capable of reproducing the starting $g(r)$.

Using Eq. (24) the function C_l is

$$C_l=2\pi\rho\int_0^\infty g(r)r^{l-2}dr$$

$$=\frac{\eta}{10d^l}\left\{\Gamma\left(\frac{l-3}{10}\right)\left[(C+1)-\frac{C}{(1-+z)^{(l-3)/10}}\right]\right.$$

$$\left.+A\left[\frac{\Gamma((m+l-3)/10)}{(1+y)^{(m+l-3)/10}}-B\frac{\Gamma((n+l-3)/10)}{(1+q)^{(n+l-3)/10}}\right]\right\}. \quad (30)$$

The results given here are for $l=12$ (corresponding to a 6-12 L-J potential); some results for $l=22$ are discussed in Appendix B.

Graphical analysis indicated that $m=16$ and $n=8$ might be close to optimum values for these parameters. Thus initial calculations were performed with m and n fixed at these values. Subsequent variation of m with n fixed at 8 yielded slightly improved results but not improved enough to warrant further calculations involving the variation of n. The final results show minimum energy for $m=6$.

The potential parameters determined by the procedure discussed in the previous section are given in Table I. In computing ϵ^* and r^* the experimental values of ρ_0 and ϵ_0 were taken to be $\epsilon_0=-0.97\times10^{-15}$ erg/atom and $\rho_0=0.0218$ Å^{-3} (see Appendix B). The quantity Q^* is a measure of the strength of the interaction and is

TABLE I. Parameters ϵ^* and r^* for a Lennard-Jones 6-12 potential.

Calculated by	ϵ^* (10^{-15} erg)	r^* (Å)	Q^* (Units of $M\epsilon^*r^{*2}/\hbar^2$)
Massey	1.409	2.974	7.434
Wu and Feenberg[a]	1.61	2.975	8.52
Hershfelder and Curtis[b]	1.411	2.869	6.96
Haberlandt[c]	1.422	2.929	7.272

[a] See Ref. 5 in text. [b] See Ref. 15 in text. [c] See Ref. 16 in text.

TABLE II. Ground-state energy per particle and optimum variational parameters as functions of density for the He^4 system.

y	q	A	d (Å)	η	z	ρ (10^{-2} Å^{-3})	$\epsilon(\rho)$ (10^{-15} erg/atom)
8.0	350	2.70	2.56	2.2925	800	2.18	−0.970
7.4	327	2.708	2.55	2.360	700	2.26	−0.967
7.0	305	2.718	2.546	2.427	610	2.34	−0.960
6.6	285	2.725	2.54	2.495	520	2.42	−0.940
6.3	267	2.737	2.535	2.56	440	2.50	−0.9125
6.0	250	2.75	2.53	2.625	350	2.58	−0.880

related de Boer's[12,13] quantum parameter which enters the theory of corresponding states. The values of ϵ^* and r^* calculated by WF[5] using the experimental $g(r)$ of Goldstein and Reekie,[14] and the values given by Hershfelder and Curtis[15] and Haberlandt[16] are also shown in Table II. In the latter two references the parameters are fixed by fitting the theoretical second virial coefficient to the observed behavior of the vapor phase.

The ground-state energy per particle $\epsilon(\rho)$ is shown in Fig. 1 as a function of density. The optimum parameters for each calculated point are given in Table II. A plot of the numbers in Table II shows that the variational parameters are smooth functions of density. Figure 2 and Table III exhibit the pressure as a function of density. The pressure curve is calculated in two ways: (a) from the relation $P=\rho^2(\partial\epsilon(\rho)/\partial\rho)$ by numerical differentiation of the $\epsilon(\rho)$ versus ρ curve of Fig. 1; (b) from the virial theorem as expressed by Eq. (20). The smooth curve comes from (a) and the points from

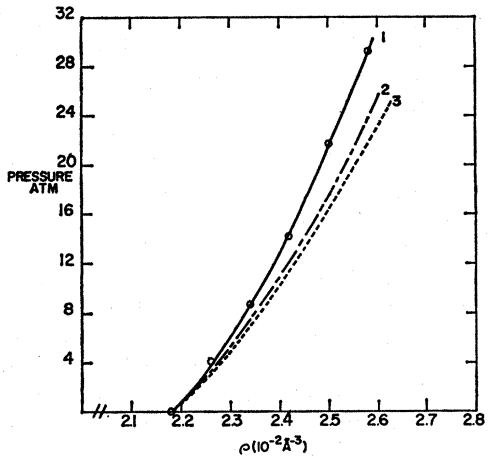

FIG. 2. The pressure as a function of density for the He^4 system, ○ = points calculated from virial theorem; (——) 1 = curve 1 obtained by numerical differentiation of $\epsilon(\rho)$ versus ρ curve; (– – – –) 2 and (– – – –) 3, experimental data from Keesom (see Ref. 17) at $T=1.25$°K and 1.75°K.

[12] J. de Boer, Physica **14**, 139 (1948).
[13] J. de Boer and R. Lunbeck, Physica **6**, 658 (1965).
[14] L. Goldstein and J. Reekie, Phys. Rev. **98**, 857 (1955).
[15] D. Hershfelder, C. Curtis, and R. Bird, *Molecular Theory of Liquids and Gases* (John Wiley & Sons, Inc., New York, 1954).
[16] R. Haberlandt, Phys. Letters **14**, 197 (1965).

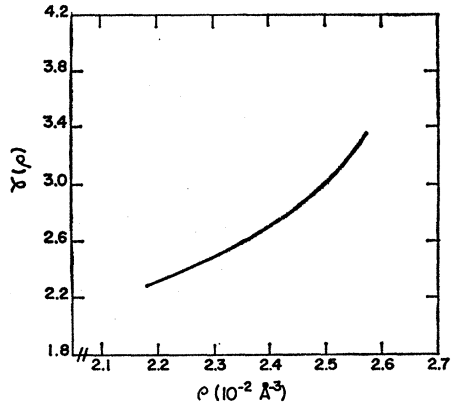

FIG. 3. Ratio of kinetic to total energy, $\gamma(\rho)=|\langle T\rangle/\langle E\rangle|$ for the He^4 system.

(b). The results from the two procedures agree to within 5% at all densities.

Also shown in Fig. 2 are the experimental data of P versus ρ for temperatures of $T=1.25°K$ and $1.75°K$ as given by Keesom.[17] There being no experimental data for lower temperatures, comparison with theory ($T=0°K$) must be semiquantitative. Between 1.25°K and 0°K, $(\partial\rho/\partial T)_P$ changes sign and becomes negative at about 1.15°K; however, the magnitude of $(\partial P/\partial T)_P$ on the lower range is small compared to its average value between 1.75°K and 1.25°K. From this it appears that the experimental P versus ρ curve at $T=0°K$ should be very close to the 1.25°K curve in Fig. 2. On this basis the theoretical results appear to decrease in accuracy as the density is raised. This is consistent with the calculated energy being too large at high densities. The calculated value of $\epsilon(\rho)$ at $\rho=0.0259$ Å^{-3} (on the melting curve) is -0.875×10^{-15} erg/atom. The experimental value is -0.917×10^{-15} erg/atom.[18]

The increase in the discrepancy between theoretical and experimental results with increasing density can be understood by noticing that a fixed relative discrepancy in $\langle T\rangle$ produces an increasing relative discrepancy in $\langle H\rangle$ as the density increases. Figure 3 shows the ratio of the kinetic to the total energy as a function of density.

TABLE III. The pressure calculated from the virial theorem and the coefficients C_6 and C_{12} as functions of density for the He^4 system.

Pressure P (atm)	Density ρ (10^{-2} Å^{-3})	C_6 (10^{-3} Å^{-6})	C_{12} (10^{-6} Å^{-12})
0.00	2.18	2.937	3.621
4.01	2.26	3.403	3.878
8.78	2.34	3.198	4.145
14.24	2.42	3.360	4.421
21.05	2.50	3.360	4.720
29.13	2.58	3.528	5.043

[17] W. H. Keesom, *Helium* (Elsevier Publishing Company, Inc., Amsterdam, 1942).

[18] K. Atkins, *Liquid Helium* (University Press, Cambridge, England, 1959).

TABLE IV. Comparison of theoretical and experimental pair-distribution functions.

Source	Temperature (°K)	Nearest-neighbor distance r_m (Å)	Height of 1st maximum $g(r_m)$	Distance of closest approach r_0 (Å)
Theoretical	0	3.48	1.31	2.18
Goldstein and Reekie[a]	2.06	3.2	1.35	2.25
Henshaw[b]	1.06	3.4	1.42	2.27

[a] See Ref. 14 in text. [b] See Ref. 25 in text.

Inaccuracies in the kinetic energy result primarily from the use of the KSA. Also the results at high densities are not expected to be as accurate as at low densities because the simple BDJ-type trial wave function does not adequately represent a system under high pressure.

The velocity of sound and the isothermal compressibility are calculated by numerical differentiation from the curve of Fig. 2. In Fig. 4 results for the velocity of sound are compared with the data of Atkins and Stasior.[18] Again the density dependence of the discrepancy between the theoretical and experimental results is apparent. At $P=0$ atm the results differ by 3.4% and at $P=25$ atm by 9.5%. The compressibility, not shown here, has the same general behavior.

The pair-distribution function for the theoretical system at $P=0$ atm is shown in Fig. 5. The experimental data of Goldstein and Reekie[14] as given by WF[5] are also shown. The Goldstein and Reekie data are for $T=2.06°K$ under normal vapor pressure. A meaningful comparison of the two curves should be limited to physically interpretable attributes. The distance of closest approach, the nearest-neighbor distance, and the relative probability of nearest neighbors (the height of the first maximum) are compared in Table IV. These quantities as given by Henshaw and Hurst[19] are also shown.

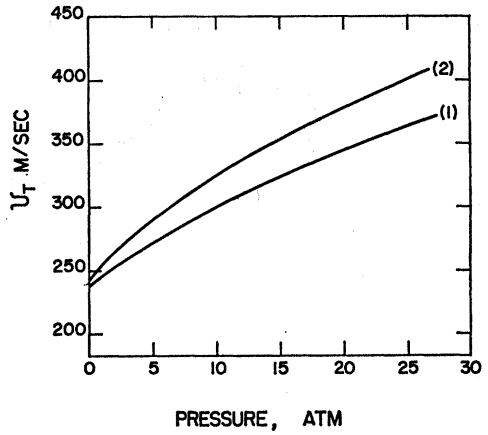

FIG. 4. The velocity of sound as a function of pressure for the He^4 system. (1) Data of Atkins and Stasior (see Ref. 18), (2) theoretical result.

[19] D. Henshaw and D. Hurst, Phys. Rev. **100**, 994 (1955).

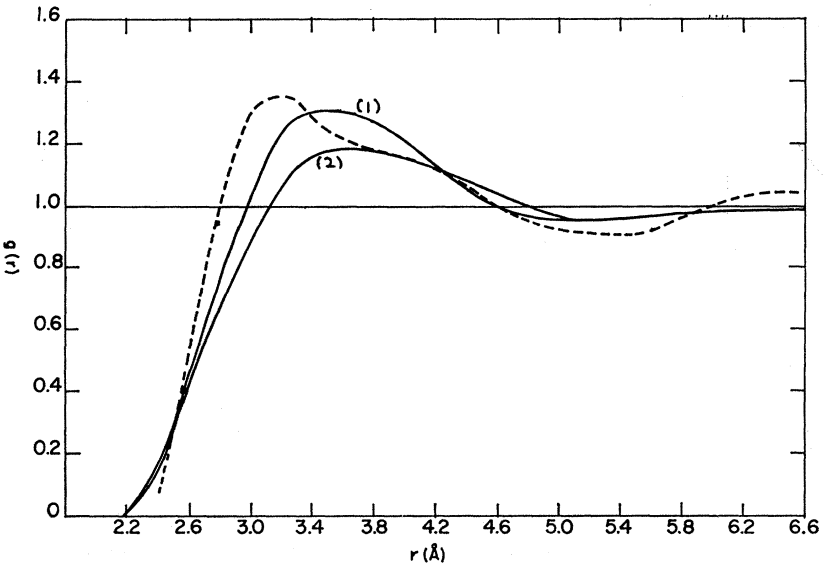

FIG. 5. The pair distribution function $g(r)$. (– – –) Represents experimental data (see Ref. 14); theoretical results for: 1 He^4, 2 the mass-3 boson system at $P=0$ atm.

Figure 6 shows the pair-distribution function at different densities. Qualitatively, the density dependence of the theoretical $g(r)$ is exactly that found experimentally by Henshaw[9] and is the expected behavior from the definition of $g(r)$. As the density increases the distance of closest approach is unchanged; the nearest-neighbor distance decreases; and the relative probability of nearest neighbors increases.

TABLE V. Results of the "Coulomb inequality" condition for He^4 and the mass-3 boson system, $Y=4\pi\rho^{2/3}\int_0^\infty [1-g(r)]r dr$.

Results for the He^4 system		Results for the mass-3 boson system	
Density, ρ (10^{-2} Å^{-3})	Y	Density, ρ (10^{-2} Å^{-3})	Y
2.18	2.584	1.64	2.466
2.26	2.587	1.80	2.515
2.34	2.602	1.96	2.556
2.42	2.610	2.12	2.585
2.50	2.615	2.28	2.594
2.58	2.617	2.44	2.599

The results for the Coulomb inequality are given in Table V. The optimum pair-distribution functions satisfy the inequality at each density.

The liquid-structure function $S(k)$ is calculated from $g(r)$ through Eq. (5). In Fig. 7 the theoretical $S(k)$ for $P=0$ atm is shown along with the experimental data of Goldstein and Reekie. The interesting portion of this curve is the region for $k\leq 0.8$ Å^{-2}. In this region experimental points are unavailable and comparison can only be made with other theoretical determinations of $S(k)$. The straight line in Fig. 7 is calculated from the Feynman formula[20]

$$S(k)\underset{k\to 0}{=}\hbar k/2MC, \tag{31}$$

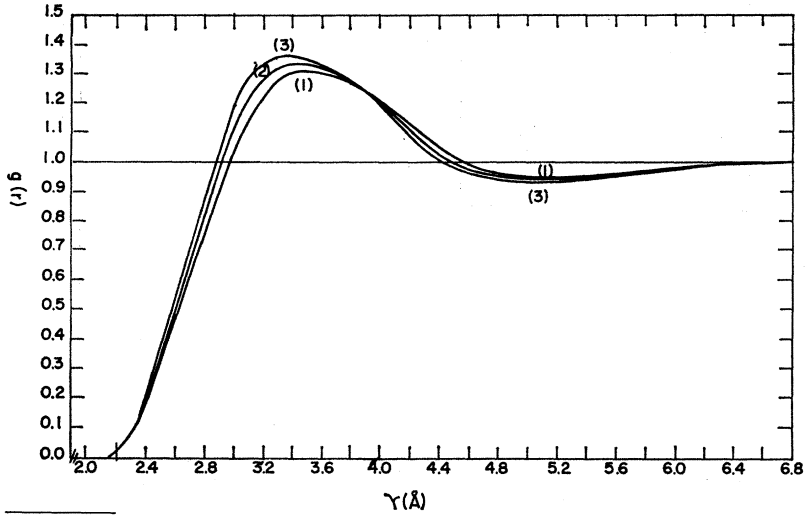

FIG. 6. The pair-distribution function $g(r)$ for different densities for He^4. (1) $\rho=0.0218$ Å^{-3}; (2) $\rho=0.0234$ Å^{-3}; (3) $\rho=0.0250$ Å^{-3}.

[20] R. P. Feynman, Phys. Rev. 94, 262 (1954).

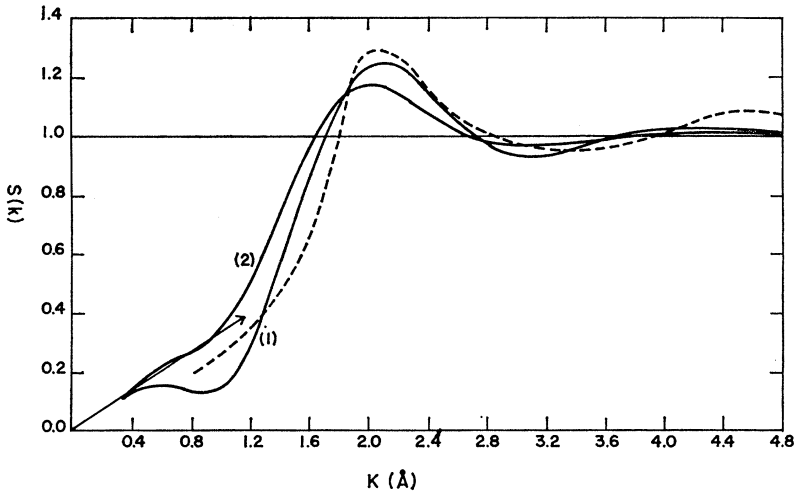

FIG. 7. The liquid-structure function $S(k)$. (----) Experimental data (see Ref. 21); (1) theoretical result for the He^4 system at $P=0$ atm; (2) theoretical result for the mass-3 boson system at $P=0$ atm; → Feynman curve.

where C is the velocity of sound. The local maximum or "shoulder" in the theoretical $S(k)$ near $k=0.6$ Å^{-1} agrees with predictions[6,21,22] based on (i) Eq. (31), (ii) the slope of the experimental $S(k)$ at $k=0.8$ Å^{-1}, and (iii) the interpretation of observed intensity relations in the inelastic scattering of slow neutrons in liquid He^4.

The theoretical curve fails to coincide with the Feynman $S(k)$ as $k\to 0$ because the theoretical $g(r)$ does not have the proper asymptotic behavior. Equation (31) has the consequence that

$$\underset{r\to\infty}{g(r)}=1-(\hbar/2\pi^2\rho MC)r^{-4}, \tag{32}$$

thus fixing the asymptotic behavior of $g(r)$.[23,24] Putting $m=4$ in Eq. (24) yields a subfamily of distribution functions with the asymptotic behavior

$$\underset{r\to\infty}{g(r)}=1+A(d/r)^m, \quad m=4. \tag{33}$$

For $A>0$ this subfamily did not satisfy the Coulomb inequality for any reasonable values of the other parameters; and furthermore solutions to the BBGKY equation were not found and also condition (29) (b), $S(k)\geqslant 0$, was not satisfied.

For $A<0$ this subfamily of trial functions satisfied all the conditions of Eq. (29) but the energy values obtained were larger than those for $m=6$. However, the trial functions are not sufficiently general to support any implication that Eq. (32) is not correct.

Any $g(r)$ with the asymptotic form given by Eq. (33) with $m>4$ will yield an $S(k)$ which is parabolic as $k\to 0$. However, the results of the present calculation (energy, etc.) are unchanged if the theoretical $S(k)$ is continued smoothly into the Feynman $S(k)$ for $k\leq 0.2$ Å^{-1}.

The appearance of the shoulder in the theoretical $S(k)$ can be understood by considering the derivative of $S(k)$ at the maximum point $k_m\approx 0.6$ Å^{-1}. Using the dimen-

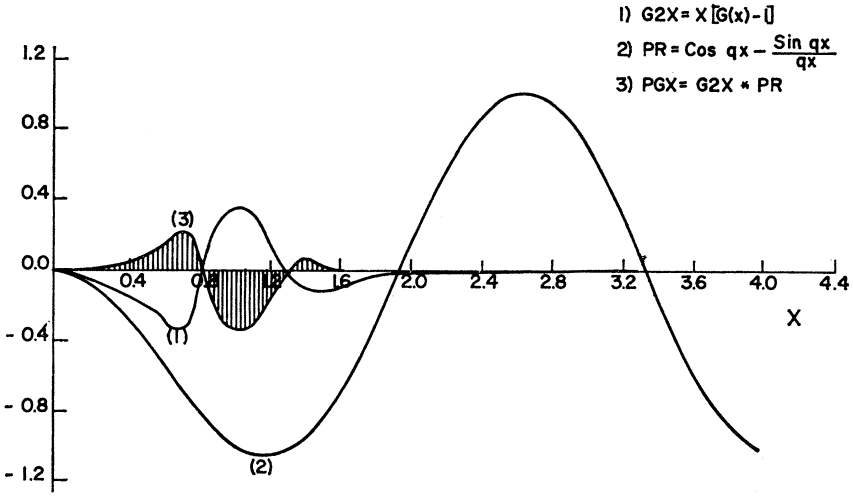

FIG. 8. Plot of integrand of

$$(\partial D(q)/\partial q)=0=2\eta \times\int_0^\infty [G(x)-1]x^2 \times[\cos qx-(qx)^{-1}\sin qx]dx,$$

$D(q)=S(q/d)$, $G(x)=g(xd)$.

[21] Allen Miller, David Pines, and P. Nozieres, Phys. Rev. 127, 452 (1962).
[22] W. E. Massey, Phys. Rev. Letters 12, 719 (1964).
[23] J. Enderly, T. Gaskell, and N. March, Proc. Phys. Soc. (London) 85, 27 (1965).
[24] E. Feenberg, in *Lectures in Theoretical Physics*, edited by W. E. Brittin and L. Marshall (University of Colorado Press, Boulder, Colorado, 1965), Vol. 7, Book C.

TABLE VI. Ground-state energy per particle as a function of density for the mass-3 boson system.

y	q	A	d (Å)	η	z	ρ (10^{-2} Å^{-3})	$\epsilon(\rho)$ (10^{-15} erg/atom)
15.00	1500	2.24	2.58	1.43	14 000	1.32	−0.3868
14.40	1330	2.29	2.58	1.505	12 300	1.40	−0.3928
13.75	1175	2.34	2.57	1.58	10 900	1.48	−0.3967
13.10	1030	2.39	2.56	1.655	9600	1.56	−0.3982
12.50	900	2.42	2.56	1.73	8500	1.64	−0.3972
11.85	800	2.47	2.55	1.80	7400	1.72	−0.3926
11.25	725	2.52	2.54	1.87	6350	1.80	−0.3830
10.70	660	2.56	2.54	1.94	5400	1.88	−0.3675
10.15	600	2.61	2.53	2.01	4500	1.96	−0.3455
9.65	550	2.66	2.53	2.08	3700	2.04	−0.3175
9.15	500	2.71	2.52	2.148	3000	2.12	−0.2840
8.75	450	2.80	2.52	2.21	2350	2.20	−0.2420
8.40	410	2.89	2.51	2.27	1900	2.28	−0.1920
8.15	380	2.99	2.50	2.33	1700	2.36	−0.1375
8.00	350	3.14	2.49	2.375	1500	2.44	−0.0680

sionless variables $x=r/d$, $q=kd$ with $G(x)=g(xd)$ and $D(q)=S(q/d)$, the derivative is written

$$\left.\frac{\partial D(q)}{\partial q}\right|_{q=q_m} = 2\eta\int_0^\infty [G(x)-1]x^2\left[\cos q_m x - \frac{\sin q_m x}{q_m x}\right]dx. \tag{34}$$

The integrand of Eq. (34) is plotted in Fig. 8. Curve (1) is the factor $x^2(G(x)-1)$, curve (2) is the factor $\cos q_m x-(q_m x)^{-1}\sin q_m x$, and curve (3) is the product of the two factors. The major contributions to the integral come from the regions in which $g(r)$ is significantly different from one. As can be seen from Fig. 8, these are the regions near the origin (the "hole"), the first maximum, and the minimum. The approach of $(g(r)-1)$ to zero cancels out long-range contributions to the integral. Thus the shoulder occurs because of the relationship between the size of the hole in $g(r)$, the height and depth of the maximum and minimum points, and the rate at which $(g(r)-1)$ approaches zero.

The density dependence of the theoretical liquid-structure function is entirely in conformity with the experimental data of Henshaw.[9,25]

The correlation function $u(r)$ is shown in Fig. 9 for two densities: the equilibrium density of the liquid;

TABLE VII. Comparison of results for the mass-3 boson system with predictions from the modified law of corresponding states.

Quantity	Corresponding-states prediction for He^3 [a]	Mass-3 boson system	% Difference
Ground-state energy per particle (10^{-15} erg/atom)	−0.208 to −0.350	−0.3983	48 to 12
Equilibrium Density of liquid (Å^{-3})	0.0182	0.01565	16

[a] See Ref. 18 in text.

[25] D. Henshaw, Phys. Rev. 119, 9 (1960).

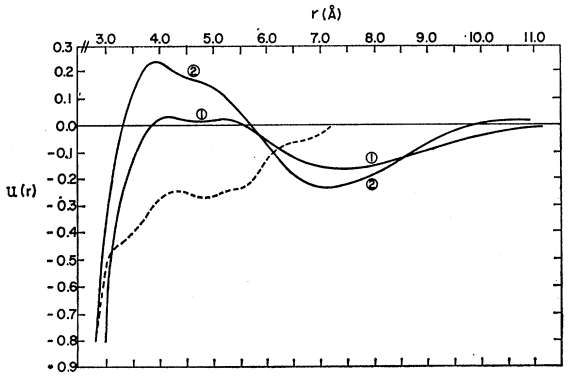

FIG. 9. The correlation function $u(r)$ for different densities for the He^4 system. (1) $\rho=0.0218$ Å^{-3}; (2) $\rho=0.0250$ Å^{-3}, (– – –) calculated by Wu-Feenberg (see Ref. 5) from experimental $g(r)$ of Goldstein and Reekie.

and a density near the experimental liquid-solid transition point for He^4. The integral term in the BBGKY equation is negligible for very small r and thus, for sufficiently small r, $u(r)$ is approximated very well by $\ln g(r)$. Since

$$g(r)\underset{r\to 0}{\sim} e^{-(d/r)^{10}}, \tag{35}$$

then

$$u(r)\underset{r\to 0}{\sim} -P/r^{10}. \tag{36}$$

The trial form

$$u(r)=-Qr^{-\nu} \tag{37}$$

has been used [in conjunction with the experimental $g(r)$ of Goldstein and Reekie] to evaluate the WF[5] functional J. Maximum J is found at $\nu=10$. This in fact is why the power of 10 was assumed in the family of trial functions used in this calculation. However, McMillan[26] and Levesque[27] using correlation functions of the form given by Eq. (37) and using Monte Carlo techniques to evaluate the many-body integrals found that the total energy was minimized by values of $\nu=5$

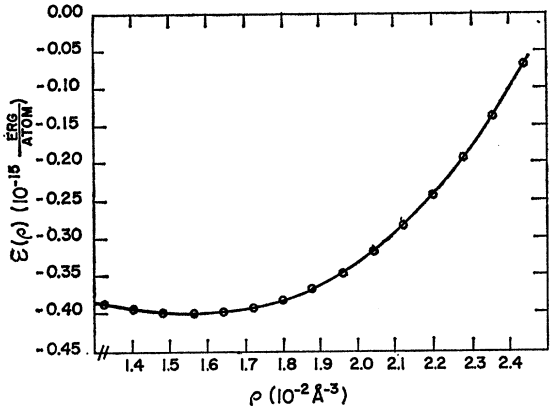

FIG. 10. The ground-state energy per particle as a function of density for the mass-3 boson system.

[26] W. L. McMillan, Phys. Rev. 138, A442 (1965).
[27] D. Levesque *et al.* (unpublished).

TABLE VIII. The pressure calculated from the virial theorem and the coefficients C_6 and C_{12} as functions of density for the mass-3 boson system.

Pressure (atm)	Density (10^{-2} Å^{-3})	C_6 (10^{-3} Å^{-6})	C_{12} (10^{-6} Å^{-12})
1.33	1.64	2.028	2.476
3.45	1.72	2.161	2.677
5.91	1.80	2.296	2.883
8.78	1.88	2.432	3.095
12.1	1.96	2.574	3.315
15.8	2.04	2.682	3.538
20.5	2.12	2.828	3.783
26.89	2.20	2.989	4.071
34.6	2.28	3.156	4.380
43.90	2.36	3.321	4.690
56.0	2.44	3.588	5.115

and $\nu=4$, respectively. Their calculations are for a finite (and small) number of particles.

The density dependence of $u(r)$ is consistent with the interpetation of $|\varphi(r_{ij})|^2=e^{u(r_{ij})}$ as a measure of the direct correlation between particle pairs.

RESULTS: MASS 3

Results for the mass-3 boson system are needed to calculate the ground-state properties of liquid He^3 by the method of correlated basis functions[3] (CBF).

Using the potential determined for He^4 [Table II] variation of the family of trial pair-distribution functions given by Eq. (24) is carried out to determine the ground-state energy and other properties of the mass-3 boson system. The calculation proceeds exactly as for He^4 except that the mass is different and the range of densities considered is different. The minimum expectation value of H is found for $m=6$ at all densities considered just as for the He^4 system. Figure 10 and Table VI give the ground-state energy per particle as a function of density. The equilibrium density has the value $\rho_0=0.01565$ Å^{-3} and $\epsilon(\rho_0)=-0.3983\times10^{-15}$ erg/atom. We can compare these results with those of de Boer and Lunbeck,[12,13] who used the Modified Law of Corresponding States (MLCS) to calculate the properties of He^3. In the MLCS calculation the effect of differing spin and statistics is neglected; hence, the results are strictly applicable to a mass-3 boson system of the type considered here. Table VII exhibits the MLCS results and those obtained here. The energy agrees fairly well but the equilibrium density obtained here is 16% lower than the MLCS value (experiment gives $\rho_0=0.0164$ Å^{-3} for He^3). The results of the CBF[3] calculation for He^3 indicate that the value of ρ_0 calculated here is indeed too small.

The pressure is given as a function of density in Table VIII and Fig. 11. As in the mass-4 calculation,

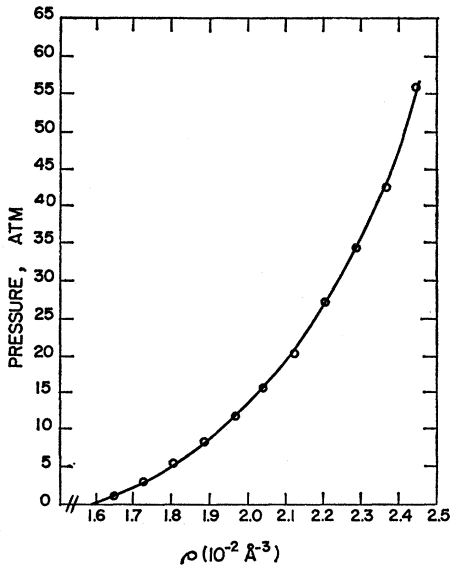

FIG. 11. The pressure versus density for the mass-3 boson system; (——) calculated by numerical differentiation of $\epsilon(\rho)$ versus ρ curve; ○=calculated from virial theorem.

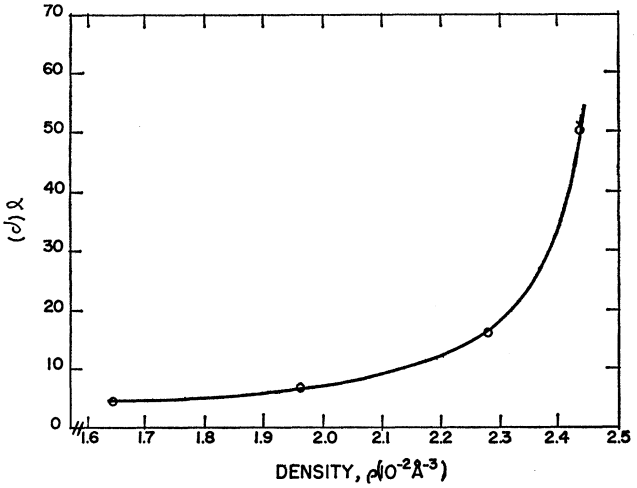

FIG. 12. The ratio of kinetic to total energy, $\gamma(\rho)=|\langle T\rangle/\langle E\rangle|$, for the mass-3 boson system.

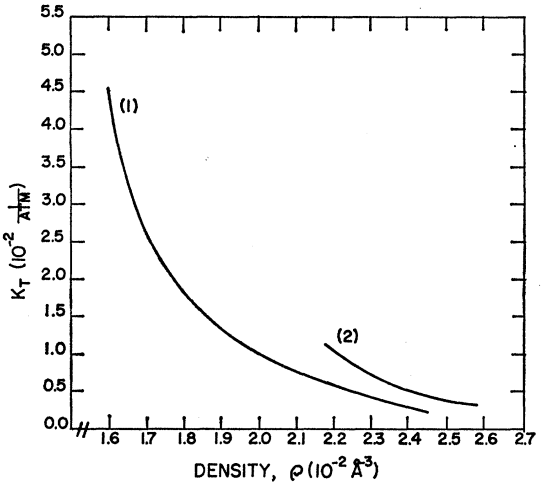

FIG. 13. Isothermal compressibility k_T versus density for (1) the mass-3 boson system and (2) the He^4 system.

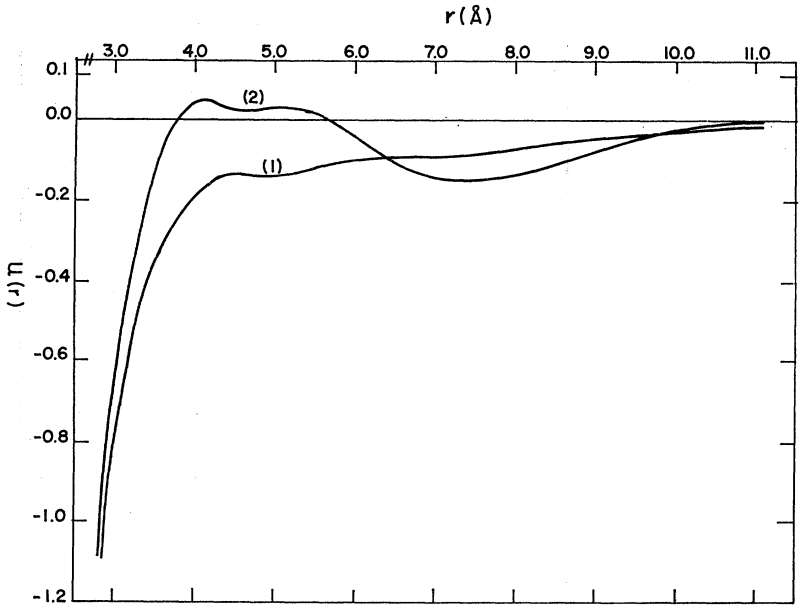

FIG. 14. Comparison of correlation functions for the mass-3 and mass-4 systems. (1) mass-3 boson system at $p=0$ atm; (2) He^4 system at $p=0$ atm.

the smooth curve is obtained by numerical differentiation and the points are calculated from Eq. (20).

The ratio of the kinetic to the total energy, $\gamma=|\langle T\rangle/\langle E\rangle|$, is shown in Fig. 12. Obviously discrepancies in the evaluation of $\langle T\rangle$ are more important for this system than for the mass-4 system. The probable error associated with large γ is discussed later.

The compressibilities of the mass-3 and mass-4 systems are shown in Fig. 13. The reduction in compressibility at a given density is a logical consequence of the increase in zero-point energy when the mass is reduced.

A comparison of the pair-distribution functions for the mass-3 and mass-4 system (at $P=0$ atm is given in Fig. 5. The differences in the functions are exactly as predicted by Ricci[28] on the basis of the MLCS; i.e., when the mass is changed from 4 to 3: (1) the effective radius of the particles is unchanged; (2) the number of nearest neighbors is reduced; (3) the distance to the nearest-neighbor shell is increased; (4) the nearest-neighbor shell is broadened.

TABLE IX. Comparison of mass-3 boson results with experimental properties of He^3.

Quantity	Mass-3 boson system	He^3 experimental
Density of liquid ($Å^{-3}$)	0.01565	0.0164
Ground-state energy per particle at $P=0$ (10^{-15} erg/atom)	−0.3983	−0.348
Compressibility at $P=0$ (atm^{-1})	5.2×10^{-2}	4×10^{-2}
Properties at density of He^3 solid; $\rho=0.0241$ $Å^{-3}$		
Ground-state energy per particle (10^{-15} erg/atom)	−0.09	−0.069
Compressibility (atm^{-1})	0.27×10^{-2}	0.35×10^{-2}

[28] F. P. Ricci, Nuovo Cimento **16**, No. 3 (1960).

The liquid-structure functions for the two systems at $P=0$ atm are compared in Fig. 7. The shoulder has practically disappeared for the mass-3 system. The CBF calculation by Woo[3] shows that the shoulder is even less apparent for He^3. Thus an experimentally verifiable prediction is made concerning the difference in the small k behavior of $S(k)$ for He^4 and He^3 near $T=0°K$.

The correlation functions for the two systems are compared in Fig. 14. The density dependence of $g(r)$, $S(k)$, and $u(r)$ is qualitatively the same for both systems.

A comparison can also be made between the calculated properties of the mass-3 boson system and the experimental properties of He^3. Table IX shows these results.

ERRORS AND APPROXIMATIONS

The use of the Kirkwood form for the three-particle distribution function is the major approximation in this calculation. The error in the results due to the KSA enters through the term J_b in the kinetic energy. [See Eq. (13).] The ratio J_b/J_{ext} gives an indication of the magnitude of this error. J_a and J_b are given for the mass-3 and mass-4 systems in Table X. Assuming that the J_b calculated here is not significantly different from its exact value, the data in Table X at $P=0$ atm permit the estimate that an error of 20% in J_b would introduce an error of only 2.9% in the kinetic energy for the mass-4 system and 2.3% for the mass-3 system. The effect on the total energy of this error goes up with increasing density. For the mass 4 system at $P=0$ atm

TABLE X. J_{ext}, J_a, and J_b as functions of density for: (A) He^4 and (B) the mass-3 boson systems.

	Density, ρ (10^{-2} Å^{-3})	J_{ext}	J_a	J_b	$(J_b/J_{ext})\times 100$
(A)	2.18	484.94	415.07	69.87	14.40
	2.34	502.86	430.87	71.97	14.31
	2.50	529.99	447.75	82.23	15.52
(B)	1.64	402.92	356.71	46.21	11.47
	1.96	430.58	374.08	56.49	13.12
	2.28	467.81	402.58	65.23	13.94
	2.44	486.74	417.89	68.85	14.14

the assumed 2.9% error in $\langle T\rangle$ causes a 6.6% error in $\langle H\rangle$. However, at $P=22$ atm a 20% error in J_b causes a 3.1% error in $\langle T\rangle$ which in turn produces an error of 9.4% in the total energy. For the mass-3 system the same trend holds.

WF,[5] using the experimental $g(r)$ of Goldstein and Reekie, found for He^4 $J_b/J_{ext}=0.065$ at $P=0$. This is about half the value of 0.144 found here. The procedure used in solving the BBGKY equation [Appendix B] defines a quantity Δ which gives a measure of the limit of error in J_{ext} due to the numerical solution of the BBGKY equation. Δ has the value 0.05%. For the mass-4 system this produces possible errors in the total energy of 0.10% at $\rho=0.0218$ Å^{-3} and 0.15% at $\rho=0.0250$ Å^{-3}. For the mass-3 system the corresponding limits of error are 0.23% at $\rho=0.0164$ Å^{-3} and 2.5% at $\rho=0.0244$ Å^{-3}.

For the mass-4 system the total error in the calculation (excluding the KSA) is estimated to be less than 1% at all densities and for the mass-3 system it is of the order of 2% at maximum.

CONCLUSION

The results of the calculation compare favorably with experiment. The density dependence of the calculated quantities is especially encouraging. Since the equilibrium point ($\rho=\rho_0$, $\epsilon(\rho_0)=\epsilon_0$) for the He^4 calculation was fixed, the results at higher densities are the true test of the calculation. Furthermore, encouraging results have been obtained for the ground-state properties of liquid He^3 using the mass-3 boson properties calculated here. Experimental data for the liquid structure function at low temperatures (<1°K) and small values of k ($\lesssim 0.6$ Å^{-1}) are needed to test some of the predictions of this calculation.

ACKNOWLEDGMENTS

I wish to thank Dr. Eugene Feenberg, who suggested this calculation and whose help was instrumental in bringing it to completion. I also wish to acknowledge the helpful assistance of C. W. Woo, H. W. Jackson, F. Y. Wu, and the staff of the Washington University Computing Center.

APPENDIX A: SOLUTION OF THE BBGKY EQUATION

The BBGKY equation is written in terms of the functional $h(r)=g(r)u'(r)$ as

$$h(r)=g'(r)-g(r)\int[g(|\mathbf{r}'-\mathbf{r}|)-1]h(r')\times\cos(\mathbf{r}',\mathbf{r})d\mathbf{r}'. \quad \text{(A1)}$$

Equation (A1) can be solved by a direct iteration process defined by the equation

$$h_{n+1}(r)=g'(r)-g(r)\int[g(|\mathbf{r}'-\mathbf{r}|)-1]h_n(r')\times\cos(\mathbf{r}',\mathbf{r})d\mathbf{r}', \quad \text{(A2)}$$

where $h_0(r)$ can be, but is not necessarily, $g'(r)$. After a certain number of iterations $h_{n+1}(r)\simeq h_n(r)$ to the required degree of accuracy.

A better method for solving Eq. (A1) uses the Wu-Feenberg extremum condition. It is clear that an optimum linear combination of functions, $h_n(r)$, $h_{n-1}(r)$, $\cdots$, $h_0(r)$, is superior as a trial solution to Eq. (A1) than any single function $h_l(r)$ ($l\leq n$). This same linear combination can also serve, when inserted in the right-hand side of Eq. (A2) in place of $h_n(r)$, to generate an improved $n+1th$ approximation. The condition for choosing the optimum coefficients in a linear combination is that the WF functional J, constructed from the trial solution, attain an extreme value.

Practical considerations limit the size of n. Here n was taken as 1 and the extreme value of J calculated as follows: Define the coefficients,

$$\mu_l=4\pi\int_0^\infty h_l(r)(g'(r)/g(r))r^2dr, \quad \text{(A3)}$$

$$\nu_{lm}=4\pi\int_0^\infty h_l(r)(h_m(r)/g(r))r^2dr+\int[g(|\mathbf{r}'-\mathbf{r}|)-1]\times h_l(r)h_m(r)\cos(\mathbf{r}',\mathbf{r})d\mathbf{r}'. \quad \text{(A4)}$$

Let $h_0(r)$ be an arbitrary approximate solution to Eq. (1). Now use $h_0(r)$ in the right-hand side of Eq. (A2) to generate the function $h_{1''}(r)$, and construct the trial solution

$$h_1(r)=(\mu_0/\nu_{00})h_0(r)+a_{1'}h_{1'}(r), \quad \text{(A5)}$$

where

$$h_{1'}(r)=h_{1''}(r)-(\nu_{01''}/\nu_{00})h_0(r). \quad \text{(A6)}$$

The WF functional J constructed from $h_1(r)$ is

$$J^{(1)}=J^{(0)}+2a_{1'}\mu_{1'}-a_{1'}{}^2\nu_{1'1'}, \quad \text{(A7)}$$

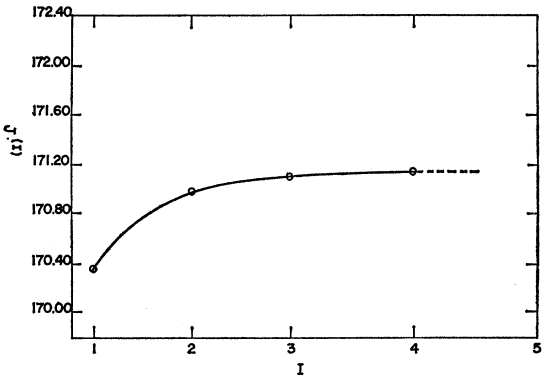

FIG. 15. Example of convergence of $J^{(I)}$ for a typical set of the variational parameters; I=No. of iteration-variation steps.

where $J^{(0)}$ is the WF functional constructed from $h_0(r)$. $J^{(1)}$ attains an extreme value for

$$a_{1'}=(\mu_{1'}/\nu_{1'1'}) \tag{A8}$$

and

$$J^{(1)}=J^{(0)}+(\mu^2{}_{1'}/\nu_{1'1'}). \tag{A9}$$

This process is repeated by using $h_1(r)$ in Eq. (A2) to generate a new function $h_{2'}(r)$ from which a new trial solution

$$h_2(r)=(\mu_1/\nu_{11})h_1(r)+a_{2'}h_{2'}(r) \tag{A10}$$

is constructed, yielding the new WF functional

$$J^{(2)}=J^{(1)}+(\mu^2{}_{2'}/\nu_{2'2'}). \tag{A11}$$

This procedure continues until $J^{(I+1)}-J^{(I)}\leq\delta$, where δ is some accepted error in the calculation. A general proof that J_{ext} is a maximum cannot be given; however, the maximum property can be proved for a special class of pair-distribution functions[29]: those subject to the condition $g(r)\leq 1$. In this calculation J_{ext} is invariably a maximum.

An example of the convergence of the $J^{(I)}$, s to a maximum value is shown in Fig. 15 for a typical set of the variational parameters. In all cases J was assumed to have reached a maximum when

$$|(J^{(I+1)}-J^{(I)})/J^{(I)}|\times 100<0.05=\Delta. \tag{A12}$$

Δ can be taken as a measure of the limit of error in the calculation of J_{ext}.

APPENDIX B: CHANGE OF ϵ_0 AND l

The experimental value of the ground-state energy per particle used in this calculation differs from that given by some other authors. The value used here, $\epsilon_0=-0.97\times10^{-15}$ erg/atom, was taken from WF.[5] Atkins,[18] Keesom,[17] and Bleaney and Simon[30] give the value $\epsilon_0=-0.9938\times10^{-15}$ erg/atom and McMillan[26] used $\epsilon_0=-0.988\times10^{-15}$ erg/atom.

Using the value given by Atkins, the results of this calculation are changed as follows: The potential parameters become $\epsilon^*=1.419\times10^{-15}$ erg (formerly 1.409) and $r^*=2.975$ Å (formerly 2.974). The new ϵ^* is closer to the values of Hershfelder and Haberlandt [see Table I]. The ground-state energy per particle for the mass-4 and mass-3 systems is shifted almost uniformly (by approximately 2%) as function of density; hence, quantities which depend on the derivative of the $\epsilon(\rho)$-versus-ρ curves (pressure, velocity of sound) are relatively unchanged. For the He^4 system $\epsilon(\rho)$ on the melting curve becomes -0.894×10^{-15} erg/atom instead of -0.875×10^{-15} erg/atom as compared to the experimental value of -0.917×10^{-15} erg/atom. Thus the discrepancy is reduced from 4.9 to 2.5%.

The ground-state energy per particle was calculated for the He^4 system using a L-J 6–22 potential. The potential parameters were determined as $\epsilon^*=2.519\times10^{-15}$ erg and $r^*=2.758$ Å. The corresponding values calculated by WF[5] using the experimental $g(r)$ are $\epsilon^*=2.608\times10^{-15}$ erg and $r=2.775$ Å. As for $l=12$, the ϵ^* given by the experimental $g(r)$ is larger and the r^*'s are about equal.

The ground-state energy is in general larger (smaller in magnitude) for $l=22$ than for $l=12$, but the difference is not significant. Thus, for the family of trial functions used here $l=12$ gives a slightly better description of He^4 at $T=0°K$.

[29] E. Feenberg (unpublished).

[30] B. Bleaney and F. Simon, Trans. Faraday Soc. 35, 1205 (1939).